Initial performance of the aspect system on the Chandra Observatory: Post-facto aspect reconstruction

Thomas L. Aldcroft, Margarita Karovska, Mark L. Cresitello-Dittmar,
Robert A. Cameron, and Maxim L. Markevitch

Smithsonian Astrophysical Observatory, 60 Garden St., Cambridge, MA, USA

ABSTRACT

The aspect system of the Chandra Observatory plays a key role in realizing the full potential of Chandra's X-ray optics and detectors. To achieve the highest spatial and spectral resolution (for grating observations), an accurate post-facto time history of the spacecraft attitude and internal alignment is needed. The CXC has developed a suite of tools which process sensor data from the aspect camera assembly and gyroscopes, and produce the spacecraft aspect solution. In this poster, the design of the aspect pipeline software is briefly described, followed by details of aspect system performance during the first eight months of flight. The two key metrics of aspect performance are: image reconstruction accuracy, which measures the X-ray image blurring introduced by aspect; and celestial location, which is the accuracy of detected source positions in absolute sky coordinates.

Keywords: Chandra, aspect, X-ray telescope

1. INTRODUCTION

Unlike the Hubble telescope, which requires very accurate pointing, the *Chandra* pointing requirements are much more relaxed. This is because *Chandra* detectors are photon counters and as long as one knows exactly where the spacecraft was pointing when each photon arrived, it is possible to determine where on the sky the photon came from. This mapping of photon positions from detector position to relative location on the sky is called image reconstruction, while the assignment of absolute sky coordinates to the image map is called celestial location. In this paper we discuss the ground software used for post-facto image reconstuction and celestial location, and give performance results based on the first eight months of flight.

The sensors on *Chandra* which are used for aspect determination are part of the Pointing Control and Aspect Determination (PCAD) subsystem. The key hardware elements which supply data used in ground processing are:

1. Aspect camera assembly (ACA) with its stray light shade

2. Fiducial light assemblies

3. Fiducial transfer system (FTS)

4. Gyroscopes (inertial reference units - IRUs)

The spatial relationship of the ACA, fid lights, and FTS is shown schematically in Figure 1. A quick overview of the hardware components is given below, but further details can be found in an accompanying paper in this volume, "Initial performance of the attitude control and aspect determination sub-systems on the Chandra Observatory" by R. Cameron, et al.
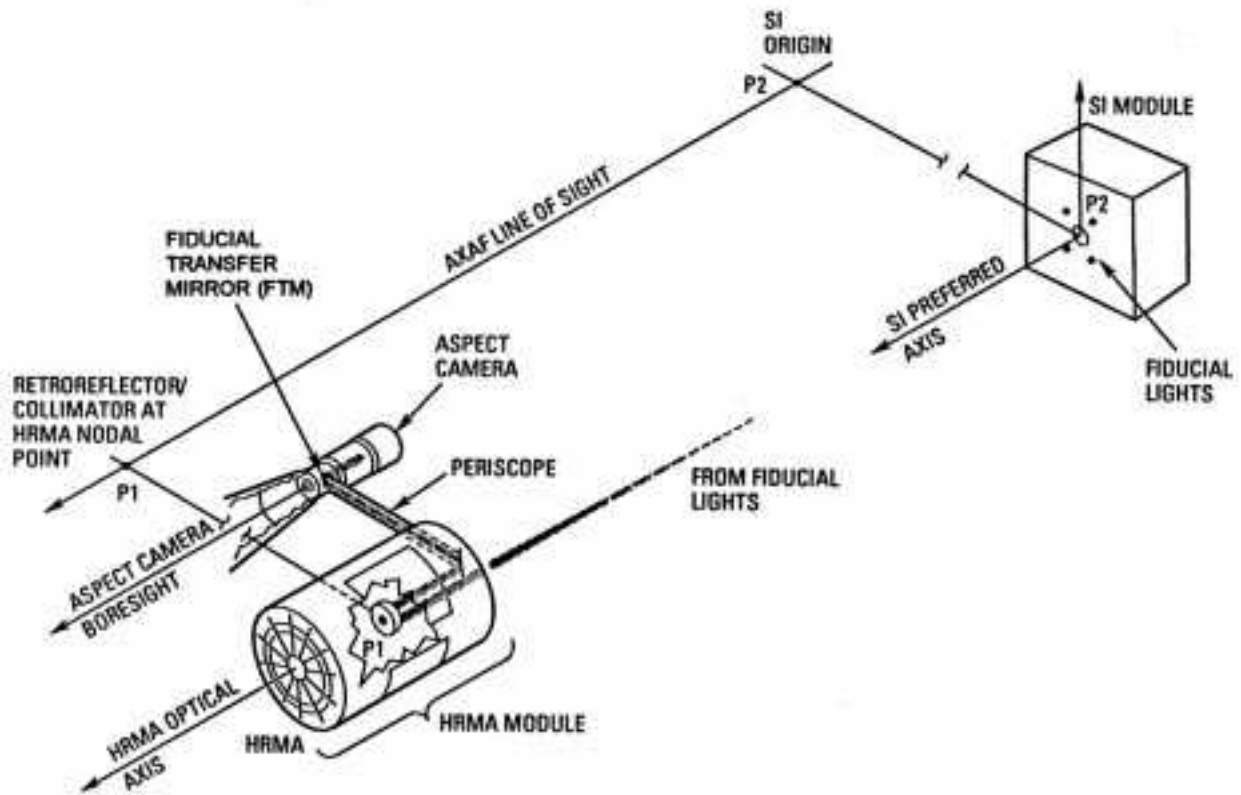
Figure 1. Aspect determination system components

The ACA serves a dual purpose: first to track stars (typically five stars with visual magnitudes between 6.2 and 10.2), and second to track the motion of the fiducial lights (typically three) which are reflected into the ACA field of view via the FTS. The external stars provide an absolute reference of the *Chandra* pointing direction, while the fiducial lights sense any bending or twisting of the telescope structure itself. Finally, the gyroscopes provide a highly accurate relative measurement of the motion of the spacecraft.

1.1. ACA

The aspect camera assembly (Figure 1) comprises a 11.2 cm, F/9 optical Ritchey-Chretien telescope. This assembly and its related components are mounted on the side of the High Resolution Mirror Assembly (HRMA). The camera's field of view is 1.4×1.4 deg. The camera itself is placed at the end of a stray-light shade, $\sim$2.5 m long, $\sim$55 cm in diameter, protecting the instrument from the light from the Sun, Earth and Moon, with protection angle of 45, 20 and 6 deg, respectively.

The aspect camera focal plane detector is a 1024×1024 Tektronix CCD chip, with 24×24 micron (5×5 arcsec) pixels, covering the spectral band between 4000 and 9000 Å. The CCD chip is deliberately out of focus (point source FWHM = 9 arcsec) to spread the star images over several pixels in order to increase accuracy of the centering algorithm, and to reduce variation in the point response function over the field of view. There is a spare identical CCD chip, which can be illuminated by activating a rotating mirror.

The ACA electronics tracks a small pixel region (either 4×4, 6×6, or 8×8 pixels) around the fiducial light and star images. There are a total of eight such image slots available for tracking. Typically there are five guide stars and three fiducial lights being tracked. On-board, the average background level is subtracted, and image centroids

are calculated by a weighted mean. The image centroids and fluxes are used by PCAD, and they are telemetered to the ground along with the raw pixel data.

1.2. Fiducial lights and Fiducial Transfer System

Surrounding each of the SI detectors is a set of 3 or 4 fiducial Light Emitting Diodes. Each fiducial light produces a collimated beam of monochromatic light (635 nm) which is imaged onto the ACA CCD via the RRC, the periscope and the fiducial transfer mirror (Figure 1). The fiducial light images are used in post-facto ground aspect determination to precisely locate the SI position relative to the HRMA optical axis.

1.3. IRU

Two Inertial Reference Units are located in the front of the spacecraft, on the side of the HRMA. Each IRU contains two gyros, each of which measures an angular rate about 2 gyro axes (X and Y). This gives a total of eight gyro channels. Data from four of the eight channels can be read out at one time. The gyros are arranged within the IRUs and the IRUs are oriented such that all 8 axes are in different directions and no three axes lie in the same plane. The gyros output pulses which represent incremental rotation angles. In high-rate mode, each pulse nominally represents 0.75 arcsec, while in low-rate mode (used during all normal spacecraft operations after orbital activation and checkout) each pulse nominally represents 0.02 arcsec.

2. ASPECT PIPELINE SOFTWARE

The essence of the ground aspect determination system is to process the sensor data from the ACA and the IRUs, and produce the aspect solution. The aspect solution consists of a time history of the absolute pointing direction (RA, Dec, and Roll) of the *Chandra* HRMA, as well as the displacement of the science instrument focal plane relative to its nominal position. As mentioned above, this displacement can occur due to bending of the spacecraft structure, and is measured via the fiducial lights.

The aspect pipeline is the suite of tools which are run as part of automatic processing and which produce the aspect solution, as well as a number of secondary aspect data products (Sec. 2.1). A tool is simply a single executable program, and the tools are called in the order specified by the aspect pipeline profile file. The inputs to each tool consist of a parameter file, which specifies various tool options or controls, and various input data files. The output of the aspect pipeline consists of the aspect data products given in Sec. 2.1.

2.1. Data products

Aspect data products are FITS files which contain aspect related data in headers, images, and binary tables. These files conform to the CXC FITS standard 2.0.0,[1] and follow the naming convention
`pcadf`<*time*>`N`<*version*>`_`<*suffix*>`1.fits`. Here <*time*> is the start time of the file, <*version*> is the reprocessing version of the file, and <*suffix*> is the data product suffix. All outputs of the aspect pipeline tools are aspect data products. A list of all aspect data products is given in Table 1.

Table 1. Aspect pipeline data products

NAME	SUFFIX	DESCRIPTION
ACACAL	acal	ACA calibration data from ODB and CALDB
ACACENT	acen	Image centroids and associated fit statistics
ACADATA	adat$<N>$	Aspect camera telemetry (including ACA housekeeping) and images for ACA image slot $<N>$
AIPROPS	aipr	Aspect intervals
ASPQUAL	aqual	Aspect solution quality indicators
ASPSOL	asol	Final aspect solution with errors
FIDPROPS	fidpr	Fidicial light properties, as commanded and as observed
GSPROPS	gspr	Guide star properties, both from the AXAF Guide and Acquisition Star Catalog, and as actually observed with the ACA
GYROCAL	gcal	Gyro calibration data from ODB and CALDB
GYRODATA	gdat	Gyro raw and gap-filled, filtered data
KALMAN	kalm	Kalman filter and kalman smoother outputs

2.2. Tools

The aspect pipeline consists of the following tools, which are called in the order given.

TOOL	INPUTS	OUTPUTS	PROCESSING
asp_read_ocat	OBSCAT	Star/fid file	Retrieve commanded guide star and fid light information for observation from Observation Catalog database
aca_id_image	Star/fid file PCADENG	GSPROPS FIDPROPS	Use PCAD engineering telemetry to check that observed star and fid positions match expectation, based on commanded values. Reject stars or fids with errors greater than 2 arcsec
asp_get_calib	PCADENG SIM CALDB	GYROCAL ACACAL	Use PCAD engineering and SIM telemetry, and the CXC Calibration Database, to assemble gyroscope and ACA calibration data appropriate for this observation
aca_read_data	ACA L0	ACADATA	Translate the ACA L0 telemetry products to the ACADATA product
gyro_read_data	PCADENG	GYRODATA	Translate the gyroscope L0 telemetry products to the GYRODATA product
asp_obc_solve	PCADENG SIM	OBCSOL	Generate a preliminary aspect solution (OBC-SOL) using attitude estimates from the PCAD subsystem of the On-Board Computer (OBC)
aca_corr_ccd	ACADATA ACACAL	ACADATA	Perform dark current subtraction and flat fielding of ACA images
aca_calc_centr	ACADATA ACACAL	ACACENT	Calculate image centroids using first moment (intensity weighted mean) and by fitting elliptical gaussians
aca_corr_centr	ACACENT ACACAL	ACACENT	Apply non-linear plate scale and color-dependent corrections to centroid values
aca_filter_centr	ACACENT	ACACENT	Reject bad centroid records (due to cosmic rays, for instance) based on iterative smoothing / sigma-reject filter algorithm
asp_corr_props	ACACENT GSPROPS FIDPROPS	GSPROPS FIDPROPS	Update the guide star and fid light properties (magnitude, position) using observed data
gyro_process	GYRODATA GYROCAL	GYRODATA	Gap-fill missing gyro data and glitches. Transform gyro rate to a 3-axis spacecraft body rotation
asp_forward_kalman	ACACENT GYRODATA ACACAL	KALMAN	Perform Foward Kalman filter on data (see Sec. 2.2.1)
asp_smooth_kalman	KALMAN	KALMAN	Perform Kalman smoothing algorithm on data to obtain attitude quaternions and gyro bias rate
asp_solve	KALMAN ACACENT FIDPROPS	ASPSOL	Transform KALMAN output to aspect solution format. Calculate common-mode motion of three fid lights and derive effective motion of SIM translation table (i.e. telescope bending)
asp_make_qualint	PCADENG ASPSOL	ASPQUAL	Determine aspect solution quality

2.2.1. Kalman filter

For the *Chandra* aspect determination problem, Kalman filtering is used to combine ACA star centroids and gyro data to determine the motion of the ACA and the gyro bias rate. A Kalman filter is the "optimal" method for estimating the state of a dynamical system given a time series of noisy measurements. It produces an unbiased estimate of the dynamical variables, along with a time-varying covariance matrix giving the estimated uncertainties. The kalman filter algorithm assumes the following about the dynamical system:

- The system is described by a linear set of first-order differential equations describing the time evolution of the state vector $\mathbf{x}(t)$

- The measured data $\mathbf{z}(t)$ are a linear combination of the state variables

- There can be random, white noise $\mathbf{w}(t)$ perturbing the dynamics

- There can be a deterministic forcing function $\mathbf{u}(t)$

- There can be random, white noise $\mathbf{v}(t)$ in the measured data

Equivalently,

$$\begin{aligned}
\mathbf{x}(t) &= \mathbf{F}(t)\mathbf{x}(t) + \mathbf{G}(t)\mathbf{w}(t) + \mathbf{L}(t)\mathbf{u}(t) \\
\mathbf{z}(t) &= \mathbf{H}(t)\mathbf{x}(t) + \mathbf{v}(t)
\end{aligned}$$

The state vector $\mathbf{x}(t)$ for *Chandra* aspect determination has six elements: three positional displacement values (effectively spacecraft roll, pitch, and yaw from the nominal pointing), and an angular three-vector giving the gyroscope bias rate. The latter term is necessary because the gyroscopes have slowly varying bias rates which need to be subtracted before integrating the gyroscope rates to obtain a positional displacement. The detailed Kalman filter equations used in the aspect pipeline are based on the formulation given in Gelb.[2]

For *post-facto* aspect determination, one can take advantage of having the full set of measurements during the entire time interval to improve the accuracy of state estimate. This involves an algorithm known as Kalman smoothing,[2] which is roughly akin to running a Kalman filter backwards through the data and combining with the forward Kalman filter estimate.

3. ASPECT PERFORMANCE

3.1. Image reconstruction

Image reconstruction is the process by which X-ray photons are assembled into an image in sky coordinates, based on the relative motion of the spacecraft. It makes no assumption about absolute position on the sky. The *Chandra* performance requirement for image reconstruction states that if the resolution and focus of the HRMA and science instruments were perfect, the reconstructed image of an X-ray point source anywhere within the central 5 arcminute radius field of view will have an RMS diameter of less than 0.5 arcsec. This translates to a one-axis 1-σ value of 0.177 arcsec.

To assess actual perfomance versus this requirement, we examine data from a *Chandra* ACIS observation of an X-ray point source. Figure 2 shows a plot of photon detector coordinate positions versus arrival time for the source. These plots show the position of photons in the ACIS CCD frame. The *Chandra* spacecraft dither pattern of ±8 arcsec is clearly visible as sinusoidal oscillations.

In Figure 3 we plot the same photon events versus arrival time, but now in aspect-corrected sky coordinates. Since the source is stationary on the sky, with perfect image reconstruction there should be no time variation in the centroid of the source in each axis. It is apparent from the plot that this is essentially the case. Quantification of the image blur introduced by aspect can, in theory, be done by calculating the source centroid as a function of time and determining any displacements from a constant. In practice this is somewhat difficult because the source count rates are low. In order to accumulate enough photons to determine a precise centroid, one typically needs to bin for a time comparable to, or longer than, the dither period of 700 to 1000 seconds. The current strategy is
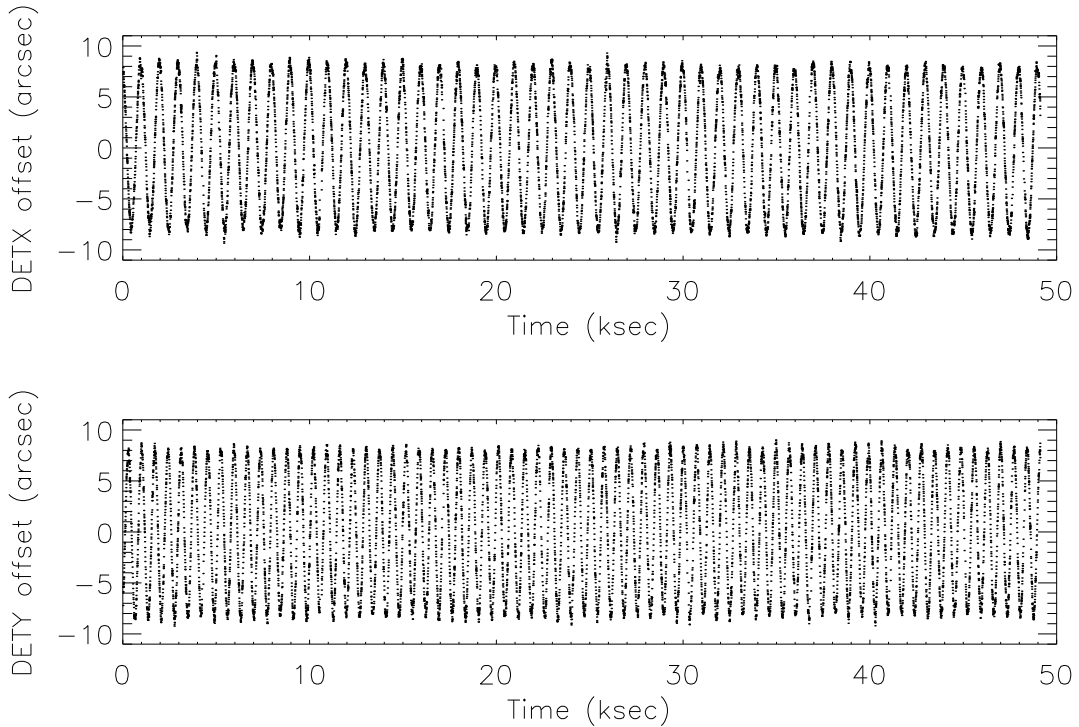
**Figure 2.** Relative detector coordinates of photons from a point source versus time

therefore to calculate an upper limit to the image reconstruction blur by binning the data into 200 second bins and calculating the RMS of centroids. This gives an upper limit to image diameter spread of 0.26 arcsec, as compared to the requirement of 0.5 arcsec.

As a final method of searching for image reconstruction errors, Figure 4 shows the combined power spectrum of the time history plots in Figure 3. This shows that the signal is essentially white noise. There is a hint a small peak in power near 700 seconds, which corresponds to one of the dither periods. However, this represents an insubstantial contribution to image diameter spread.
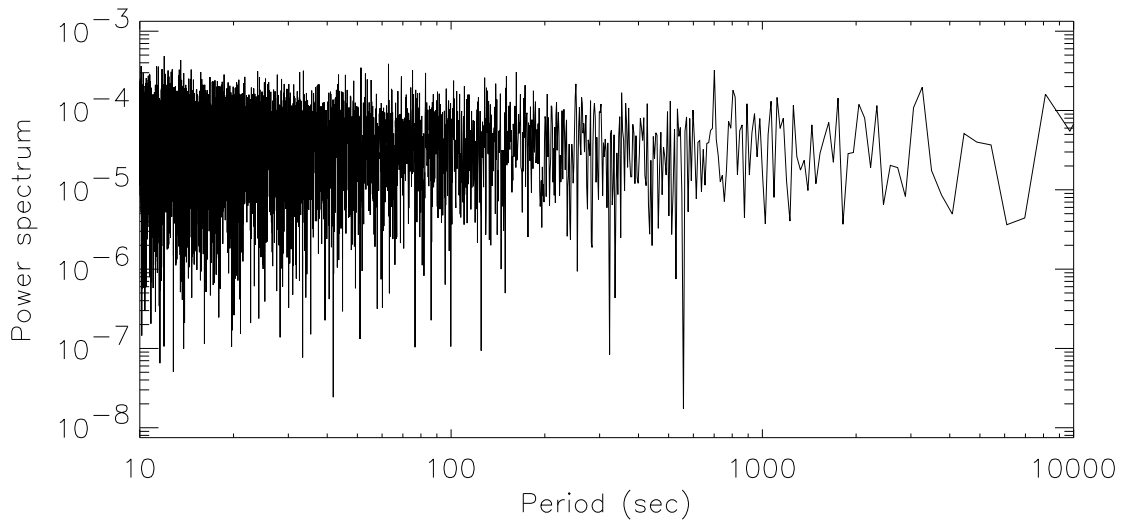
3.2. Celestial location

Celestial location refers to the absolute accuracy with which a reconstructed image can be placed on the celestial sphere. The project requirement specifies that the radial errors in derived X-ray source coordinates must have an RMS of less than 1.0 arcsec.

The key element of celestial location determination is the boresight calibration. This allows us to specify the relationship between observed position of an X-ray source on the detector, observed star positions in the ACA, and observed fiducial light positions in the ACA. In order to fully constrain the problem, at least two X-ray sources, two stars, and two fiducial lights are needed. Conceptually, boresight calibration is simplest if the X-ray sources are also imaged in the optical with the ACA. In practice this is not required, nor feasible, and instead we have used the star cluster NGC 2516. This has many X-ray sources with well-measured optical counterparts (which are too faint for the ACA). The ACA instead tracks normal guide stars with magnitudes in the range 6.2 to 10.2, as well as the fiducial lights. Using the simultaneous observation of X-ray sources, optical stars, and fiducial lights, we then calculate two alignments: (1) ACA alignment relative to the HRMA optical axis reference frame; and (2) FTS relative to the HRMA frame. The second alignment term is effectively to null out any offsets in fiducial light positions due to misalignments in the FTS optics (retro-reflector collimator and periscope).
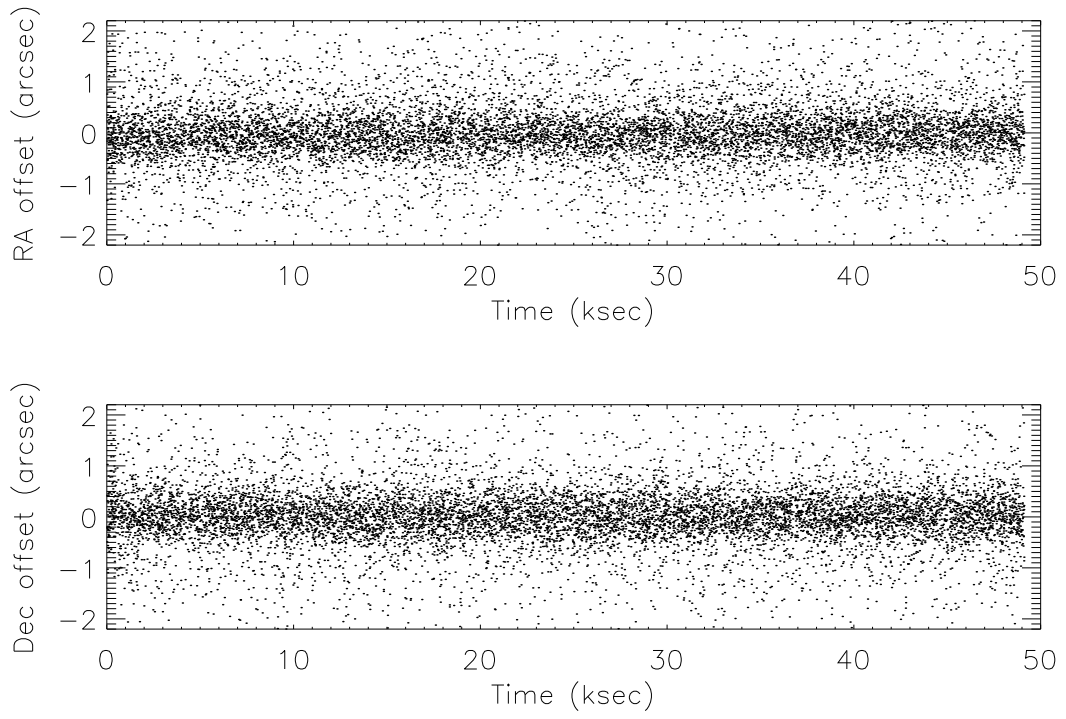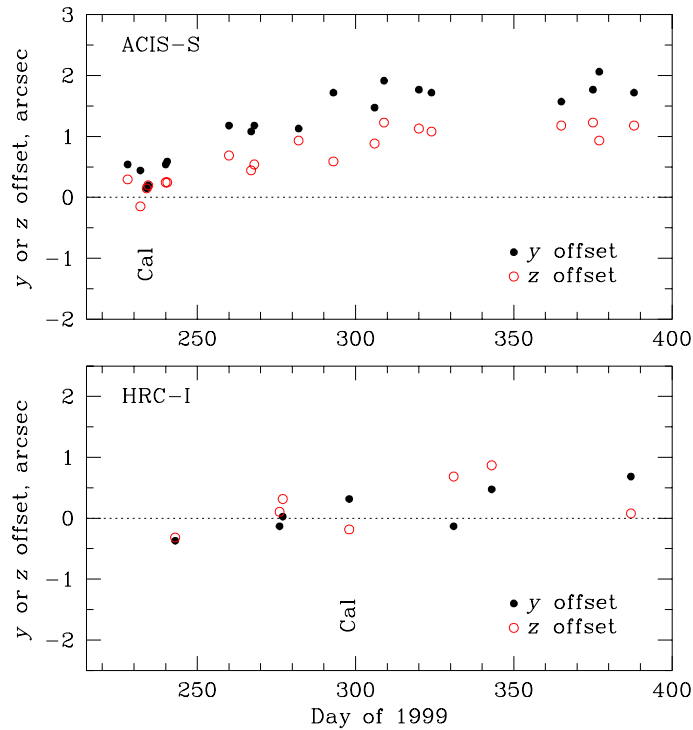
Figure 3. Relative sky coordinates of photons from a point source versus time

Figure 4. Power spectrum versus period for point source observation

Figure 5. Long term drift in celestial location error

To check the actual performance versus the requirement, we require observations of point sources which have an optical or radio counterpart with accurately known positions. Unfortunately, the astrometry in many common source catalogs is not accurate at the sub-arcsecond level, even in cases where precision to 0.1 arcsec is indicated. Therefore we restricted the possible source list to those found in the International Celestial Reference Frame catalog.[3]

Figure 5 shows plots of celestial location errors for a number of observations, versus time. The date of boresight calibration measurements for HRC and ACIS are marked on the plots. For HRC-I (bottom), the celestial location accuracy is about 0.6 arcsec RMS radius, and meets requirements. However, for observations with ACIS-S, there was a steady drift between day 220 to day 310 of 1999, followed by a constant offset up to the present. The physical cause of this apparent drift is unknown at this time. To compensate for this drift, the CXC will implement a time-varying boresight calibration for ACIS-S based on these observed offsets. When this long-term drift is removed, the RMS celestial location error for ACIS-S is less than 0.5 arcsec.

ACKNOWLEDGMENTS

REFERENCES

1. http://icxc.harvard.edu/icd/FITS/ascfits2.0.ps
2. A. Gelb, *Applied Optimal Estimation*, M.I.T. Press, Cambridge, MA, 1974.
3. Ma et al. 1998, Astrophysical Journal 116, 516.